

PAPER • OPEN ACCESS

Analysis on the impact characteristics of grounding device considering spark effect

To cite this article: Hengzhen Li *et al* 2020 *J. Phys.: Conf. Ser.* **1585** 012003

View the [article online](#) for updates and enhancements.

You may also like

- [Research on Performance of Grounding Conductor Based on Multi-Physics](#)
Sun Xiangdong, Ding Hui, Cui Jinrui *et al.*
- [Application and Implementation of The Grounding Wire Information Management System Based on SM2](#)
Jiajun Liu and Xueli Liu
- [Acoustic guided wave detection of grounding rod corrosion: equivalent circuit model and implementation](#)
Nicholas Durham, Junhui Zhao, Gregory Bridges *et al.*



ECS
The
Electrochemical
Society
Advancing solid state &
electrochemical science & technology

DISCOVER
how sustainability
intersects with
electrochemistry & solid
state science research

Analysis on the impact characteristics of grounding device considering spark effect

Hengzhen Li^{1*}, Zilan He¹, Sixiang Chen¹, Ming Zhang¹, Yingjun Shu¹ and Chen Hu²

1 Foshan Power Supply Bureau of Guangdong Power Grid Co., Ltd, Foshan, Guangdong 528011, China

2 School of Electrical Engineering, Southwest Jiaotong University, Chengdu, Sichuan 611756, China

* Correspondence: 1041175958@qq.com

Abstract. Under the effect of lightning current which is with large amplitude, the grounding device and surrounding soil will have spark effect, which makes device show complex impact characteristics and affect the current dissipation process. In this paper, using the parallel plate device, the quantitative relationship between the resistivity of sandy and brown yellow soil and the field strength is obtained, which is expressed as a piecewise function. Considering this relationship, a finite element model of impact dissipation for grounding device is established. A test platform is built, and the impact test data of different topological forms is used to compare with the results of the model, which can verify that the model can effectively analyse the spark effect of the grounding body. After carrying out simulation for the grounding body of different topological forms, this paper analyses the impact dissipation characteristics of the horizontal grounding body and the grounding body with short conductors.

1. Introduction

Lightning current flows into the ground through lightning wire and transmission tower when they are struck by lightning. When the current dissipation reaches a certain strength, spark discharge occurs in the soil, which has an impact on the whole dissipation process, making the impact grounding resistance of grounding device drop and operation of the transmission line safer [1-3].

The research on the soil impact characteristics is significant to the lightning protection of power grid. According to the research, the breakdown of soil is related to its resistivity, when resistivity is in the range of 20-1000 $\Omega \cdot m$, the critical breakdown field strength of the soil is 300 kV/m [4]. Nor N. M. Obtained the curve of voltage and current at the time of breakdown by the breakdown experiment, and calculated the breakdown field strength of soil by comparing the simplified method [5-6].

This paper obtains the critical breakdown field strength of typical soils and the relationship between the resistivity of sandy and brown yellow soil and the field strength by impact tests. Based on the test data, the model taking account of spark effect is established by using COMSOL multiphysics, and it is verified using tests. The impact characteristics of the two topologies including horizontal grounding body and grounding body with short conductors are studied by the established model.

2. Soil impact test

In order to obtain the impact characteristics of soil under different field strength, this paper needs to carry out impact tests on different soil. The device includes high-voltage impact generator which can

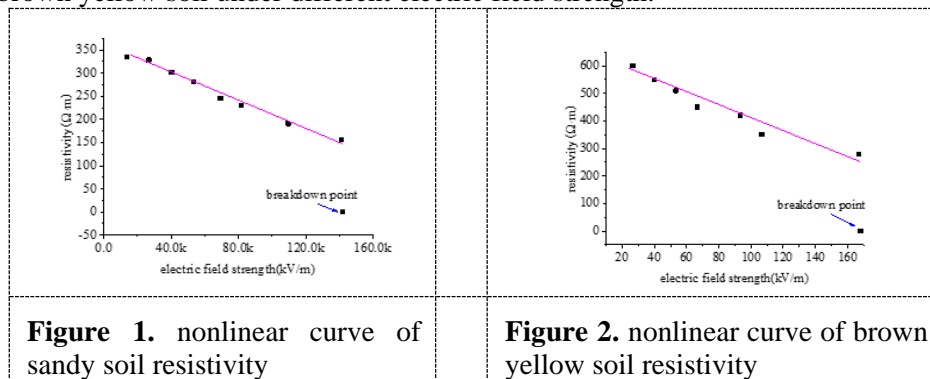


generate 8/20 μ s impact voltage, rogowski coil and parallel plate device. The soil samples to be tested are filled in the parallel plate of the acrylic box, which can be considered that the field strength between the plates is basically the same. After a series of experiments, the breakdown field strength of different soil with different water content is obtained, as shown in table 1:

Table 1. breakdown field strength of different soils

sandy soil		brown yellow soil		red soil		yellow soil	
water content (%)	breakdown field strength (kV/m)	water content (%)	breakdown field strength (kV/m)	water content (%)	breakdown field strength (kV/m)	water content (%)	breakdown field strength (kV/m)
6.82	141	6.31	167	5.75	428	7.5	337
12.15	114	9.8	141	10.45	241	11.42	224
19.3	111	19.06	123	18.1	188	20.1	163
26.5	106	27	116	29.1	135	26.7	125

Subsequently, more detailed tests are carried out on the two soils with large porosity differences, i.e. sandy soil and brown yellow soil. The water content of two soils samples are 6.82% and 6.31% respectively, and the resistivity under normal conditions is 335 $\Omega\cdot$ m and 700 $\Omega\cdot$ m respectively. In order to fully recover the soil to ensure the accuracy of the test, the interval after each discharge is more than 20min. The applied voltage of each test and the current flowing through the electrode plate is recorded to calculate the soil resistivity. figure 1 and figure 2 show the nonlinear curve of the resistivity of sandy and brown yellow soil under different electric field strength.



It can be seen from the above data that with the increase of applied voltage, the resistivity of sandy soil and brown yellow soil decreases slowly. When the voltage is applied to a certain extent, the soil is finally broken down by electric field. At this time, the field strength of two soils is 141.3kV/m and 167.0kV/m respectively. Due to the great breakdown current, its value is not obtained in the test. So according to the research of relevant scholars, the resistivity after breakdown is 7% of the original resistivity [7-8]. Using curve fitting of the results, the relationship between the resistivity of sandy soil and brown yellow soil and the field strength (respectively ρ_{1x} and ρ_{2x}) can be obtained as follows:

$$\rho_{1x} = \begin{cases} \rho_{10} & E < 26.8 \text{ kV/m} \\ (1.1 - 0.005E)\rho_{10} & 26.8 \text{ kV/m} \leq E < 141.3 \text{ kV/m} \\ 7\% \rho_{10} & 141.3 \text{ kV/m} \leq E \end{cases} \quad (1)$$

$$\rho_{2x} = \begin{cases} (0.94 - 0.0036E)\rho_{20} & E < 167.0 \text{ kV/m} \\ 7\% \rho_{20} & 167.0 \text{ kV/m} \leq E \end{cases} \quad (2)$$

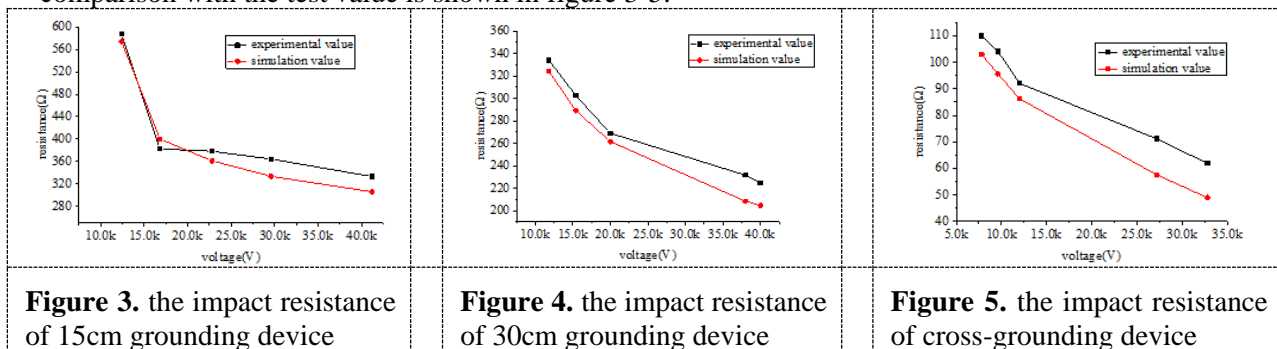
In formulas (1) and (2), ρ_{10} and ρ_{20} are the normal resistivity of sandy and brown yellow soil respectively, and E is the applied electric field strength.

3. Establishment and verification of the impact dissipation model

In this paper, COMSOL multiphysics is used to establish the finite element model of the grounding body. The area for the soil current dissipation is set to be hemispherical, and the size of the hemispherical is much larger than the grounding conductor. Because the power source is the impact source, the "transient" study is selected. According to the experiment in the previous chapter, under the impact current, the resistivity of soil around the grounding conductor changes in different degrees.

In order to verify the correctness of the above model, this paper will use a hemispherical sand pond with a diameter of 5m to test the spark effect of the soil, and compare the results with the established model. In the test, the conductors are horizontal grounding devices with a length of 15cm and 30cm and 1.5m*1.5m cross grounding device, and the diameter of round steel is 5mm. the buried depth of the conductor is 10cm, and the soil resistivity is $352\Omega\cdot\text{m}$ during the test.

According to the test parameters, the dissipation model of hemispherical sand pond is established, and a single conductor is located in the centre of sphere. the soil type in the sand pond is sandy soil, so the relationship between the soil resistivity and the field strength is constructed by using formula (1), and ρ_{10} is $352\Omega\cdot\text{m}$. According to the parameters used in the test, the model calculates the impact resistance of the grounding device when the length is 15cm, 30cm and the cross-grounding device, and the comparison with the test value is shown in figure 3-5.



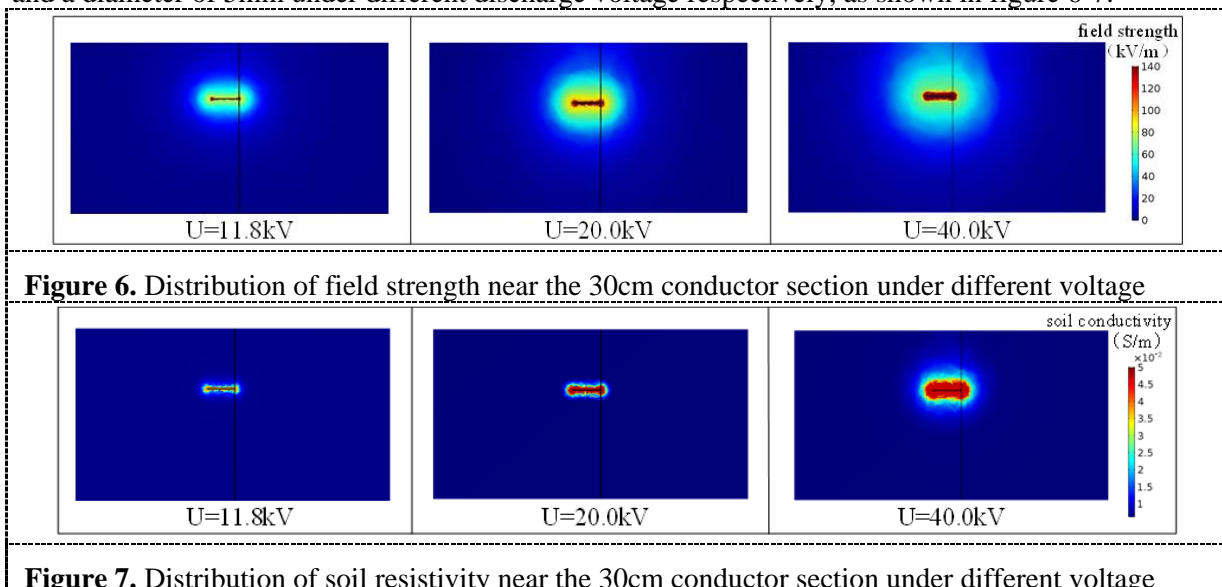
Through the comparison of test and simulation, it can be seen that the error between the conductor impact impedance calculated by using the grounding body impact dissipation model considering spark effect established in this chapter and the test value is within 8%, indicating that the model can be used to restore the dissipation of the grounding device when spark effect occurs.

4. Analysis of impact characteristics of different grounding bodies

The topological structure of transmission line tower grounding device is various. In this chapter, based on the consideration of spark effect, the dissipation characteristics of two topologies are studied.

4.1. Single horizontal grounding body

According to model in chapter 3, the impact characteristics of horizontal grounding body under different voltage levels can be analysed. Selecting the peak time of impulse current, this paper draws the distribution of field strength and soil resistivity near the conductor section with a length of 30cm and a diameter of 5mm under different discharge voltage respectively, as shown in figure 6-7.



In the simulation, with the increase of voltage, the spark effect of soil becomes more obvious. The soil resistivity around the grounding body changes regularly in an ideal state, and the spark shape in the simulation is similar to the concentric cylinder. But in the actual experiment, the spark shape of soil is affected by some factors of soil such as looseness and impurities, so the actual spark shape is not regular. As a result, the simulation value of impact resistance is slightly less than the test.

It can be seen from figure 6 that the field strength at both ends of the grounding device is significantly greater than that in the middle of the grounding device. When the electric field strength of the surrounding soil reaches a certain value, the soil will have different degrees of partial ionization and spark area. In figure 7, the spark area generally starts at the end of the conductor section, and it spreads to the middle when voltage becomes high. The spark area increases with the growth of the voltage, which can be equivalent to the increase of the radius of the grounding device. It is not hard to find that the trend of spark distribution is similar to that of field strength distribution.

The simulation also calculates the distribution of soil resistivity when the length is 15cm, as shown in figure 8. Through the comparison, the shorter the conductor section is, the greater the surrounding field strength is, the more concentrated the spark area is. combining with figure 3-5, the impact resistance of the 15cm long conductor is 574Ω at 12.8kV, and when the impact voltage reaches about 40kV, the impact resistance decreases by 50%, while 30cm long conductor is 35%, which is because the longer the conductor is, the larger the area of current dissipation is, and the less concentrated the field strength is. So, the spark effect will occur more likely under the same impact voltage, and the impact resistance will drop more faster during the growth of voltage when the conductor is shorter.

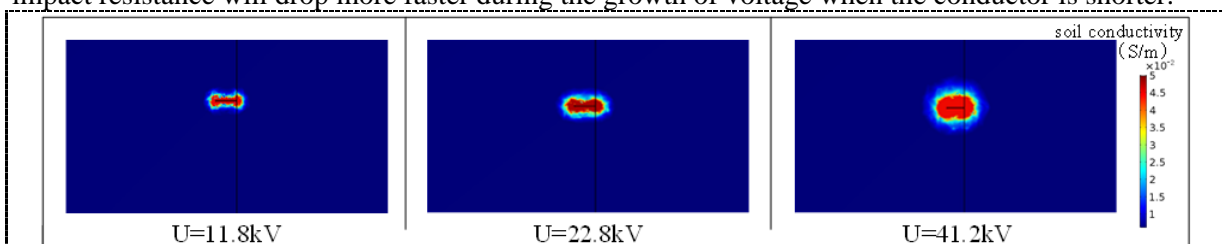


Figure 8. Distribution of soil resistivity near the 15cm conductor section under different voltage

4.2. Grounding body with short conductors

Horizontal grounding with short conductors is commonly used in practical engineering. The length of short conductors in this calculation is 40cm, and distance between conductor referred as d is divided into four situations: 5cm, 10cm, 20cm and 30cm. The length of horizontal conductor is 1.5m, and the diameter is 5mm. impact dissipation characteristics are analysed from the following three aspects.

From the potential distribution diagram in figure 9, it can be seen that the potential distribution is more uniform and the potential is more concentrated with the increase of d . Combined with figure 10 and figure 11, it is apparent that when $d=30\text{cm}$, there is no obvious shielding effect between the conductor sections. When the distance is further shortened, the current dissipation between the conductor will affect each other and have obvious shielding effect. And with the decrease of distance, the area of sparking area around the conductor decreases, which leads to the increase of impact resistance.

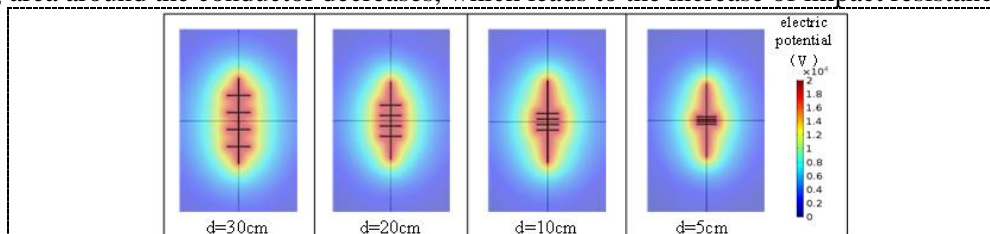


Figure 9. Potential distribution of grounding body with short conductors

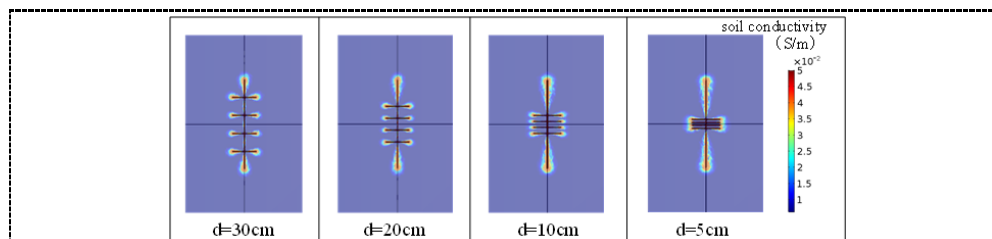


Figure 10. soil resistivity distribution of grounding body with short conductors

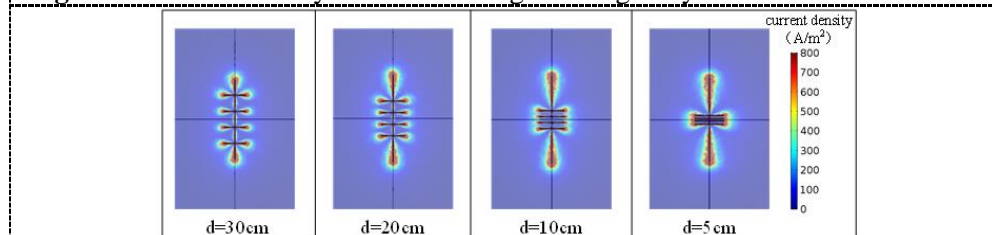


Figure 11. current density distribution of grounding body with short conductors

5. Conclusion

In this paper, a dissipation model of grounding device considering spark effect is established. The conclusion is as follows: Comparing the results of model with the sand pond test, it is found that they are in good agreement, which means this model can be used to restore the current dissipation when the spark effect occurs. According to the simulation of grounding bodies, for the horizontal conductor, the spark area first appears at the end and extends to the middle with the increase of voltage; compared with conductor of 15cm and 30cm, the shorter the conductor is, the stronger the spark effect is under the same voltage; for grounding body with short conductors, shorter distance between short conductors will cause more concentrated peripheral potential and larger impact resistance.

6. Acknowledgments

Thanks for the support by the Guangdong Power Grid Limited Liability Company, Foshan Power Supply Bureau. The study is supported by the science and technology project of Guangdong Power Grid Limited Liability Company of China (Item Number: GDKJXM20182401).

7. References

- [1] Qi Lei, Cui Xiang, Zhao Zhibin, et al. Grounding performance analysis of the substation grounding grids by finite element method in frequency domain[J]. IEEE Transactions on Magnetics, 2007, 43(4): 1181-1184.
- [2] Jinliang He, Baoping Zhang, and Rong Zeng. Experimental studies of impulse breakdown delay characteristics of soil[J]. IEEE Transactions on Power Delivery, 2011, 26(3): 1600-1607.
- [3] Anton H., Mladen T. The simulation of the soil ionization phenomenon around the grounding system by the finite element method[J]. IEEE Transactions on Magnetics, 2006, 42(4): 867-870.
- [4] Mousa A. M. The soil ionization gradient associated with discharge of high currents into concentrated electrodes[J]. IEEE Transactions on Power Delivery, 1994, 9(3): 1669-1677.
- [5] Nor N. M., Haddad A., Griffiths H. Determination of threshold electric field E_c of soil under high impulse currents[J]. IEEE Transactions on Power Delivery, 2005, 20(3): 2108-2113.
- [6] Nor N. M. Ionisation gradient of low resistivity soils and liquids[C]. Electromagnetic Compatibility, 2006. EMC-Zurich 2006. 17th International Zurich Symposium on Singapore, 2006: 409-412.
- [7] M. Mokhtari, Z. Abdul-Malek and Z. Salam. An Improved Circuit-Based Model of a Grounding Electrode by Considering the Current Rate of Rise and Soil Ionization Factors[J]. IEEE Transactions on Power Delivery, 2015, 30(1): 211-219.
- [8] M. Laboda, Z. Pochanke, Experimental study of electric properties of soil with impulse current injections[C], 18th ICLP Munich, 1985, 191-198.